Supporting Information

Selenylsulfide Bond-Launched Reduction-Responsive Superparamagnetic Nanogel Combined of Acid-Responsiveness for Achievement of Efficient Therapy with Low Side Effect

Yanan Xue[1§], Xiaoyang Xia[1§], Bo Yu[1], Lijun Tao[1], Qian Wang[2], Shi-Wen Huang[2], Faquan Yu[1*]

[1] *Key Laboratory for Green Chemical Process of Ministry of Education*

Hubei Key Laboratory for Novel Reactor and Green Chemistry Technology

School of Chemical Engineering and Pharmacy,

Wuhan Institute of Technology, Wuhan 430073, China

[2] *College of Chemistry and Molecular Sciences*

Wuhan University, Wuhan 430072, China

[§] These authors contributed equally to this work.

[*]Corresponding author:

Faquan Yu, Professor, PhD

Wuhan Institute of Technology

Xiongchu Ave 693, Wuhan 430073, Hubei, China

E-mail address: fyu@wit.edu.cn

Tel: (86-27) 87194980; Fax: (86-27) 87194465

Experimental section

1 Materials

Sodium alginate (SA, Mw=32-250 kD), cysteamine hydrochloride (98%), N-(3-dimethylaminopropyl)-N'-ethylcarbodiimide hydrochloride (EDC, 98%), N-hydroxysuccinimide (NHS, 98%), 3-chloropropionic acid (98%) and sodium borohydride ($NaBH_4$, 98 %) were purchased from Aladdin Industrial Co. 3,3'-Dithiodipropionic acid (DTDPA, 99%), potassium hexacyanoferrate (II) trihydrate (98.5%), potassium thiocyanate (KSCN, 99%), parafor-maldehyde (95%), hoechst 33258, and 3-[4,5-dimethyl-thiazol-2-yl]-2,5-diphenyltetrazoplium bromide (MTT) were purchased from Sigma-Aldrich. Dimethyl sulfoxide (DMSO), selenium powder (99%), and dialysis tubing (MWCO 8000-14000) were purchased from Sinopharm Chemical Reagent. Doxorubicin hydrochloride (DOX·HCl, 98 %) was purchased from Arking Pharma Scientific. All chemicals were used as received without further purification. Ultrapure water was prepared by Heal Force super NW water purification system (Heal Force Development Ltd.).

HeLa, L02 and H22 cell lines were purchased from Chinese Typical Culture Center (CTCC, Wuhan University) and cultured in RPMI-1640 medium (Gibco) supplemented with 10% fetal bovine serum (FBS, Hyclone) and 1% antibiotics (100 U mL^{-1} penicillin and 100 mg mL^{-1} streptomycin) at 37 $^{\circ}$C in a humidified atmosphere containing 5 % CO_2.

2 Instruments

Fourier transform infrared (FTIR) spectra were recorded on a Nicolet 5700 spectrometer in the wavenumber range of 400-4000 cm^{-1}. Samples were ground with KBr and pressed to plates for measurement. ^{1}H nuclear magnetic resonance (^{1}H NMR) spectra were recorded on a Bruker Avance-500 spectrometer using D_2O as solvent. The size, size distribution, and zeta potential were investigated by dynamic light scattering (DLS) using a Zetasizer (Malvern Nano-ZS90) with a He-Ne laser beam at 633 nm at 25℃. Morphology of nanocarrier was observed under a transmission electron microscope (TEM) using Tecnai G2S-Twin at an accelerating voltage of 200 kV. Around 5μL of the nanocarrier suspension was placed on a copper grid. The grid was allowed to dry at room temperature overnight. The magnetic property of DOX-loaded nanocarrier was evaluated on a vibrating sample magnetometer (VSM, Westerville, OH, USA) via changing the magnetic field from -20000 to 20000 Oe at 25℃.

3 Synthesis of 3, 3'-diselanediyldipropanoic acid (DSeDPA)

3, 3'-Diselanediyldipropanoic acid (DSeDPA) was synthesized according to previous reports with some modifications [1-2]. Selenium powder (3.95 g, 50 mmol) in 25 mL of ice water with NaOH (2.0 g, 50 mmol) was added to a three-necked flask under a nitrogen atmosphere. $NaBH_4$ (0.25 g, 6.6 mmol) and NaOH (0.20 g, 5 mmol), previously dissolved in 5 mL of ice water, were syringed dropwise into the selenium suspension. The mixture reacted at 0℃ with agitation until color faded completely. The mixture was then heated to 90 ℃ until reddish brown appeared.

3-Chloropropanoic acid (5.42 g, 50 mmol) was dissolved in 20 mL of water, and its pH was adjusted to 8.0 with Na_2CO_3. This was added to the reddish brown solution above and stirred overnight at room temperature under N_2. The reaction mixture was filtered, and the yellow supernatant was adjusted to pH 3-4 using 1 mol L^{-1} HCl and extracted twice with ethyl acetate. The organic layers were washed with water, dried with anhydrous magnesium sulfate, and finally recrystallized to give a yellow product of 2.5 g (32.9% yield).

4 Synthesis of selenylsulfide bond modified alginate (SA-SSe-COOH)

SA-SSe-COOH was synthesized by the exchange reaction between the sulfhydryl group of thiloated alginate (SA-SH) and the diselanediyl group of DSeDPA [3]. SA-SH was synthesized following previous work by amidation reaction between cysteamine and sodium alginate (SA) [4]. The modification degree of the pendent SA-SH, defined as the percentage of the glucose unit that has been substituted with functional SH groups (coded as x in Fig 1A), was determined to be 16.2% by the Ellman's method. DSeDPA (0.1g, ~0.3 mmol) in 30 mL phosphate solution (0.01 mol L^{-1}, pH 6.5) was added to a three-necked flask under a nitrogen atmosphere. SA-SH (0.125 g) dissolved in 30 mL phosphate solution (0.01 mol L^{-1}, pH 6.5) was syringed dropwise into the above solution. The reaction mixture was stirred at 37 °C for 7 h. The resultant solution was dialyzed against ultrapure water and finally lyophilized to obtain SA-SSe-COOH as yellow powder. The chemical structure of SA-SSe-COOH was confirmed by ^{1}HNMR.

5 Preparation and fluorescence labeling of magnetic DOX-loaded nanogel containing selenylsulfide bond (MDSeSAN-gel)

Aminated SPION (SPION-NH_2) was first prepared following our previous work [5]. The average hydrodynamic size was determined to be 21.6±1.7 nm with zeta potential of +28.3±0.4 mV. MDSeSAN-gel was prepared through the electrostatic interaction between the carboxylic groups of SA-SSe-COOH and the amino groups on DOX/SPION-NH_2. In a typical procedure, SPION-NH_2 (4 mL, 1.25 mg mL^{-1}) with 0.25 mg of DOX was added dropwise to SA-SSe-COOH solution (5 mL, 1 mg mL^{-1}). The suspension was stirred for 2 h at room temperature and then transferred into a dialysis bag (MWCO 14000) to dialyze against ultrapure water and freeze-dried to obtain MDSeSAN-gel, which was stored in 4 °C until further use. The nanogel was then labeled with fluoresceinamine isomer according to the method published previously [6-7]. Plain nanogel or DOX-free nanogel was prepared following the above procedure with the exception of DOX.

6 *In Vitro* DOX release

The in vitro release behavior of MDSeSAN-gel was investigated in phosphate solution at different pH and GSH conditions using a dialysis-diffusion method. Briefly, 2 mL suspension of MDSeSAN-gel was introduced into a dialysis bag (MWCO 14000), which was immersed into 18 mL PBS (0.01 mol L^{-1}) at pH 7.4 or pH 5.0 without or with 10 μmol L^{-1}/10 mmol L^{-1} GSH. The release experiment was

conducted in a water bath with a shaking rate at 60 rpm at 37 °C. At predetermined intervals, 3.0 mL of the incubated solution was taken out and replaced with 3.0 mL of corresponding fresh buffer solution. The amount of DOX released was determined at 490 nm by fluorescence spectrometer. All measurements were performed in triplicate. Drug loading content (DLC) and drug loading efficiency (DLE) were calculated according to the equation as follows:

$$\mathrm{DLC}(\%) = \frac{\text{weight of loaded drug}}{\text{total weight of lyophilized nanogels}} \times 100\,\%$$

$$\mathrm{DLE}(\%) = \frac{\text{weight of loaded drug}}{\text{weight of drug in feed}} \times 100\,\%$$

7 *In Vitro* cytotoxicity assay

The in vitro cytotoxicity was measured in HeLa and L02 cell lines by MTT assay. Cells were seeded into 96-well flat-bottomed plates at a density of ~5000 cells per well in 100 μL complete RPMI-1640 containing 10% FBS and cultured for 24 h at 37 °C in 5% CO_2 atmosphere before test. Then, cells were treated with 100 μL of plain nanogel or MDSeSAN-gel or DOX that was serially diluted in complete RPMI 1640 medium at different concentrations. As a control, 100 μL solution of fresh complete RPMI-1640 medium without any MDSeSAN-gel or DOX was applied. After 12 h、24 h or 48 h of incubation, the culture medium was disposed and cells were washed thrice with PBS (0.01 mol L^{-1}, pH 7.4). Subsequently, 100 μL culture medium and 10 μL MTT solution (5 mg mL^{-1} in PBS) were added to each well with further incubation for 4 h. The medium was then removed and 200 μL of DMSO was added to dissolve

formazan crystal. In the above procedure, blank wells were designed by substituting PBS solution for MTT solution. The absorbance was measured at a wavelength of 570 nm using a microplate reader (Macromolecule Devices SpectraMax M2e).

External magnetic field was investigated as an additional factor on the cytotoxicity. A permanent magnet was placed beneath the 96-well plate for 4 h incubation. After the removal of the magnet and washing thrice with PBS, identical amount of fresh medium was loaded for another 12 h, 24 h or 48 h incubation. The control experiments were carried out without the application of magnet.

The relative cell viability (%) in reference to control wells was calculated according to the equation:

$$\text{Relative cell viability}(\%) = \frac{\text{Absorbance of sample} - \text{Absorbance of blank}}{\text{Absorbance of control} - \text{Absorbance of blank}} \times 100\,\%$$

Relative cell viability graphs were plotted against DOX concentrations for convenient comparison. Data were presented as average ± SD (n=8).

8 Cellular uptake

8.1 Prussian blue staining

Prussian blue staining was used as a qualitative and visual method to observe the intracellular iron distribution [8]. HeLa cells were seeded into 24-well plates at a density of ~5 x 10^4 cells per well in 1 mL complete RPMI-1640 containing 10% FBS and cultured for 1 day at 37 °C in 5% CO_2 atmosphere. Then, the culture medium was replaced with 1 mL of fresh medium containing 225 μg mL^{-1} plain nanogels. For control cells, no nanogels were applied. After 24 h incubation, the cells were washed

thrice with PBS (0.01 mol L^{-1}, pH 7.4) and fixed for 10 min using 4% (w/v) paraformaldehyde at room temperature. After washed thrice with PBS, the cells were stained with 1 mL of freshly prepared 4% potassium ferrocyanide and 8% HCl solution for 30 min at 37 °C. Finally, the stained cells were washed thrice with PBS and visualized by a reverse microscope (Ti, Nikon, Japan).

8.2 Confocal laser scanning microscopy (CLSM) observation

CLSM was employed to visualize the intracellular distribution of DOX. In brief, HeLa cells were seeded in a glass bottom cell culture dish with 2mL of RPMI-1640 growth medium at a density of ~2×10^5 cells per well. After 24 h of incubation at 37 °C, The attached cells were then incubated with MDSeSAN-gel and maintained in a cell culture dish for another 4 h or 24 h at 37 °C. The final concentration of DOX, calculated out in terms of the DLC value of the nanogel, was set at 0.30 μg mL^{-1}. At predetermined time, the cell monolayers were then rinsed triple with PBS (0.01 mol L^{-1}, pH 7.4), fixed with 4% (w/v) paraformaldehyde at room temperature for 10 min, and then again washed with PBS triple. To label nuclei, fixed cells were incubated with Hoechst 3325 solution (5 mg mL^{-1} in PBS, 0.2 mL $well^{-1}$) at 37 °C for 10 min and then washed with PBS three times. Finally, the prepared slides were analyzed by CLSM (Nikon, TE2000, EZ-C1, Japan).

9 *In Vivo* antitumor efficacy

All animal experiments were performed in compliance with the guidelines approved by the committee of Wuhan University on Use and Care of Animals. The tumor

growth inhibitory activities of MDSeSAN-gel were assessed in BABL/c mice following reported methods [9] (female 5-6 weeks old, animal experiment center of Wuhan university, China). To establish the H22 tumor model, H22 mouse liver cancer cells (~1×10^7 cells mL^{-1}, 0.1 mL) were subcutaneously injected into the femoribus internus of BABL/c mice. When tumors grew to an average volume of about 100 mm^3, the mice were randomly divided into three groups (n=5), and intravenously administered via tail vein weekly with sterile PBS, DOX·HCl and MDSeSAN-gel at a dose of 3.3 mg (DOX) per kg (body weight), respectively. The body weight of the mice and tumor size were monitored every other day. At day 21, the mice were sacrificed by cervical decapitation and their tumor volume and weight were measured. The developed tumor was monitored with a caliper in two dimensions and calculated using the following formula [10]:

$$V = \frac{\text{the longest diameter of tumor} \times (\text{the shortest diameter of tumor})^2}{2}$$

The tumor size was expressed as an arithmetic means with a standard error.

The tumor growth inhibition rate (IR) was calculated as follows [11]:

$$IR(\%) = 1 - \frac{\text{weight of tumor in the experimental group}}{\text{weight of tumor in the control group}} \times 100\%$$

10 Histological analyses

The tumors and major organs (heart, liver, spleen, lungs and kidneys) were excised, weighed and then fixed in 4% PBS buffered paraformaldehyde overnight and then embedded in paraffin. The paraffin embedded tumors and organs were cut at 5 μm thickness and stained with hematoxylin-eosin (H&E) and with prussian blue for

pathological examination and histological alterations assessment by a microscope (Olympus IX51 / Q-IMAGING Micro Publisher).

Supplementary figures

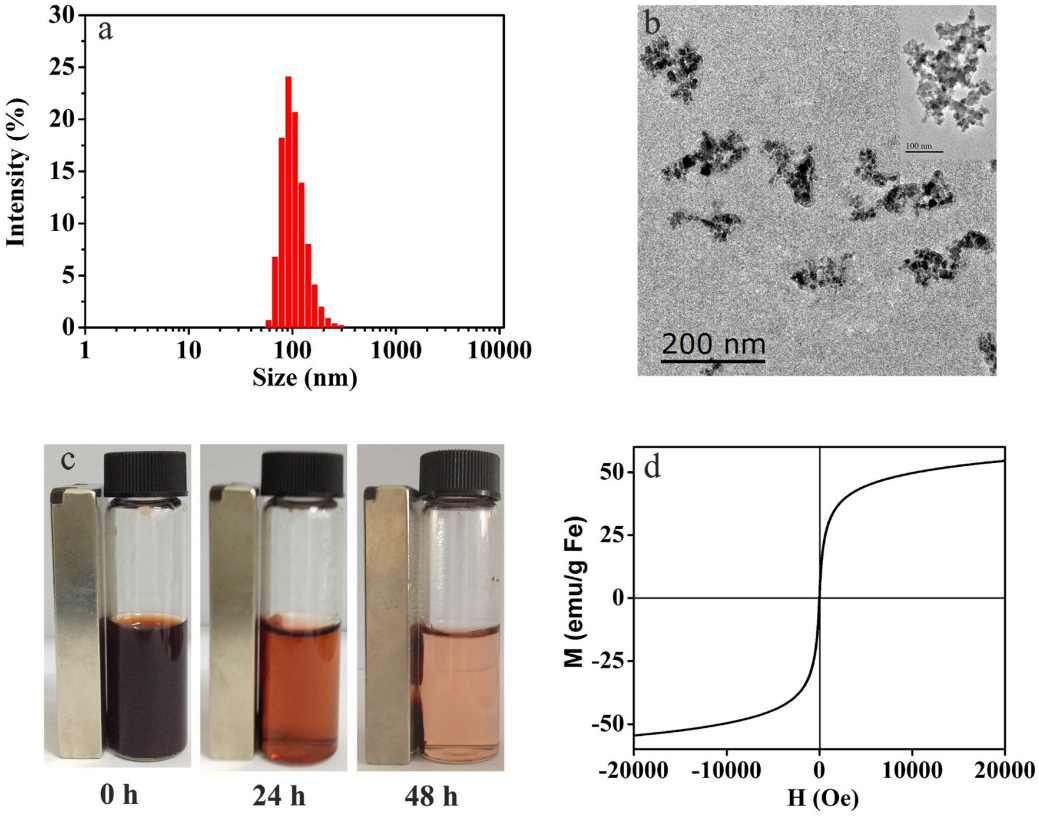

Fig S1. The size distribution of MDSeSAN-gel by DLS (a), TEM images (b), visual observation of magnetophoresis exposed to a magnet for 0 h, 24 h and 48 h (c), and vibrating sample magnetometer profile of the magnetic MDSeSAN-gels (d).

The DLS average size was approximately 105 nm with a polydispersity index of 0.165 and the zeta potential at -44.2±0.7 mV. The DLS size was consistent with that of TEM images. The TEM images indicated that the nanogel is an aggregate containing many small and dark particles. Each aggregate is considered as a single nanogel though it is hard to completely exclude the possibility of the existence of

aggregation of more than one nanogel. First, the coating shell can help effectively to judge the individual particle. Second, the aggregated image size matches the DLS result. Third, there are such mechanisms to assemble or crosslink the principal SPIONs into a larger particle or the final nanogel, shown in Fig S1. Additionally, other researchers reported the similar images [12-13]. The irregular morphology is in agreement with previous observation [14-15].

The magnetophoresis was clearly displayed in light of the visual variation in color after exposed to magnet. The VSM results demonstrated that MDSeSAN-gel exhibited superparamagnetic properties, without remnant hysteresis loop observed in the magnetization/demagnetization curves. The saturation magnetism for the MDSeSAN-gel was estimated to be 53.4 emu/g Fe.

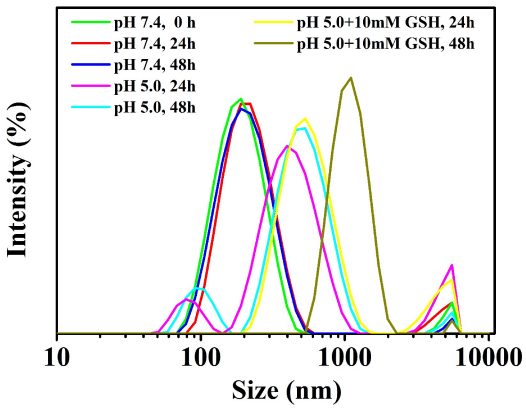

Fig S2. The size change of MDSeSAN-gel exposed to different environments: 0.01 mol L^{-1} PBS of pH 7.4 and pH 5.0 with or without 10 mM GSH for different time.

Both the size and the size distribution varied slightly during the period of 48 h in pH 7.4 PBS buffer, even showing slight variation over two weeks. Due to the copious

carboxylic groups pending on alginate, the carboxylic groups left after the conjugation with DOX or SPION-NH_2 made the resultant nanogel negatively charged. The strong surface charge allows the nanogel long storage stability.

When exposed to pH 5.0, the size increased and precipitate was observed after 48 h. The mildly acidic medium neutralizes the carboxylic group-orginated negative surface charge on the nanogel and thus attenuates electrostatic repulsion, which leads to coagulation or accounts for the increased size. When 10 mM GSH was applied in pH 5.0, a notably increased size was observed. In fact, the observation showed actual precipitation after 48 h. As well, GSH would induce the cleavage of selenylsulfide bond. Both of the mechanisms will bring about the disassembly of the nanogels, which elucidated the occurrence of small size peak.

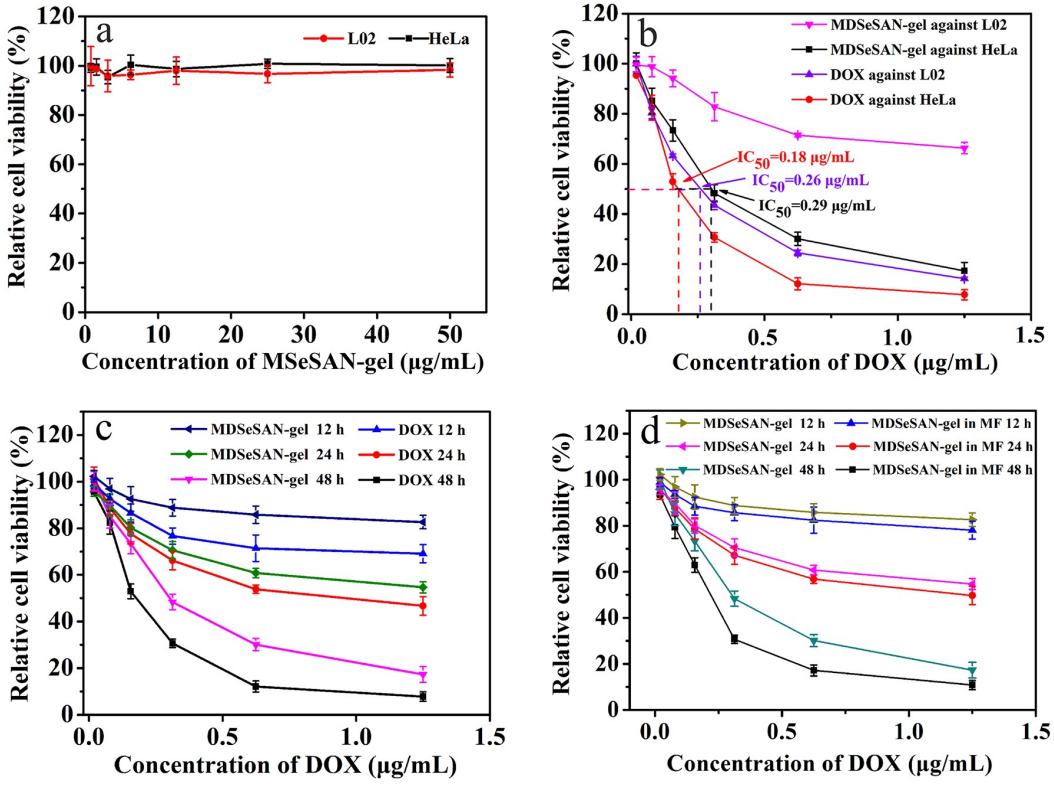

Fig S3. Cytotoxicity comparison of (a) plain nanogel between against HeLa and L02

cell lines after 48 h incubation, (b) free DOX and MDSeSAN-gel between against HeLa and L02 cell lines after 48 h incubation, (c) free DOX and MDSeSAN-gel against HeLa cell lines dependent on incubation time, (d) MDSeSAN-gel against HeLa cell lines dependent on external magnetic field (MF: magnetic field).

The half maximal inhibitory concentration (IC_{50}) of MDSeSAN-gel against HeLa was 0.29 μg mL^{-1}, an equivalent inhibition effect with free DOX (IC_{50}=0.18 μg mL^{-1}). In comparison to the IC_{50} (0.26 μg mL^{-1}) of free DOX，the L02 cell viability of MDSeSAN-gel was up to 88% at the same dose. No IC_{50} of MDSeSAN-gel was observed in the range of tested concentrations. Theoretically, the cytotoxicity is closely related with the released DOX from the nanogel. The reduced cytotoxicity indicated the DOX release in the healthy cell lines was retarded seriously. The cell viability of MDSeSAN-gel decreased from 82.6%, 54.7% to 17.3% with the increase of incubation time from12 h, 24 h to 48 h, compared with 68.0% (12 h) , 46.4% (24 h) and 8.0% (48 h) at the same dose of free DOX (1.25 μg mL^{-1}), respectively. The cell viability was also tested with external magnetic field, shown in Fig S3d.

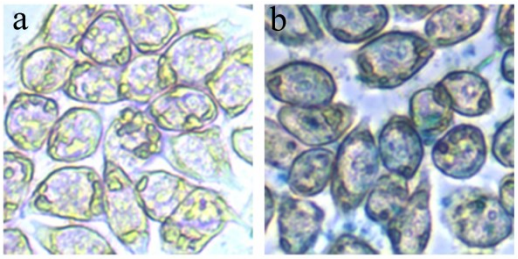

Fig S4. Microscopic images of Prussian blue stained iron in HeLa cells treated by plain nanogels (b) in contrast with the untreated (a). The images were obtained at

200× magnification.

The cellular uptake and intracellular distribution of iron and DOX were evaluated with HeLa cells with Prussian blue staining, as shown in Fig S4. After incubation with the plain magnetic nanogel for 24 h, HeLa cells were stained with potassium ferrocyanide and visualized by a reverse microscopy. The number of blue granules significantly increased when the magnetic nanogel was applied, compared with the untreated group. This implies that the MDSeSAN-gel could be rapidly endocytosed by HeLa cells.

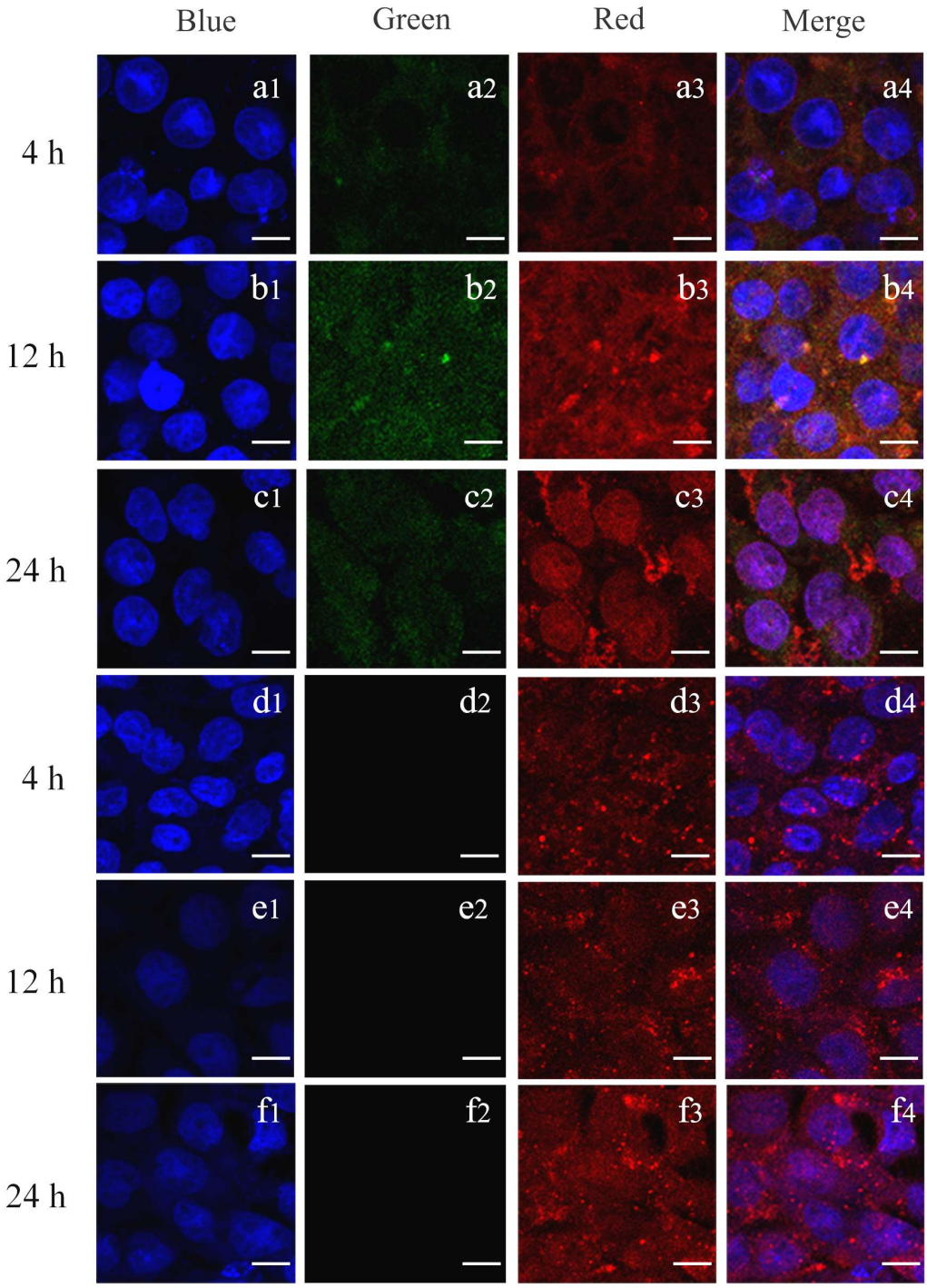

Fig S5. CLSM images of HeLa cells treated with MDSeSAN-gels (a-c) and free DOX (d-f) for respective 4 h, 12 h and 24 h incubation. Blue is cell nucleus treated with Hoechst; Green is alginate treated with Fluoresceinamine; Red is DOX fluorescence; the last column is their overlap. The bar is 20 μm.

To further demonstrate whether MDSeSAN-gel can be more efficiently internalized by HeLa cells, experiments on the intracellular study of fluoresceinamine isomer labeled MDSeSAN-gel were performed on HeLa cells after treatment for 4, 12 or 24 h using CLSM analysis. Blue color is the cell nucleus treated with Hoechst 33258 and green and red colors are the fluorescence of fluoresceinamine and DOX, respectively. As shown in Fig S5, strong DOX fluorescence was observed in the cells after 4 h incubation with free DOX. With increase of the incubation time, more evident DOX was visualized in both cytoplasm and nuclei. In contrast, cells incubated with MDSeSAN-gel for 4 h showed both weak DOX and fluoresceinamine isomer fluorescence in the cytoplasm and little was observed in nuclei area, indicating the nanogel plays a role to restrict the release of DOX due to the encapsulation of DOX inside the nanogel. Both DOX and fluoresceinamine (representing alginate) fluorescence intensity increased with the incubation time. DOX was observed in nuclei after 12 h of incubation and the accumulation became more evident there, indicating the enhanced endocytosis of nanogels and the subsequent transfer of released DOX inside the cytoplasm into the nuclei. It is suggested that the mild acid environment in cytoplasm dissociated the electrovalent bonds between the negative carboxyl group and the positive amine group as well as high intracellular GSH concentration caused the cleavage of the selenylsulfide linkage. As a result, the nanogel disassembled and led to accelerate the release of DOX, resulting in the rapid localization of DOX in the cell nucleus.

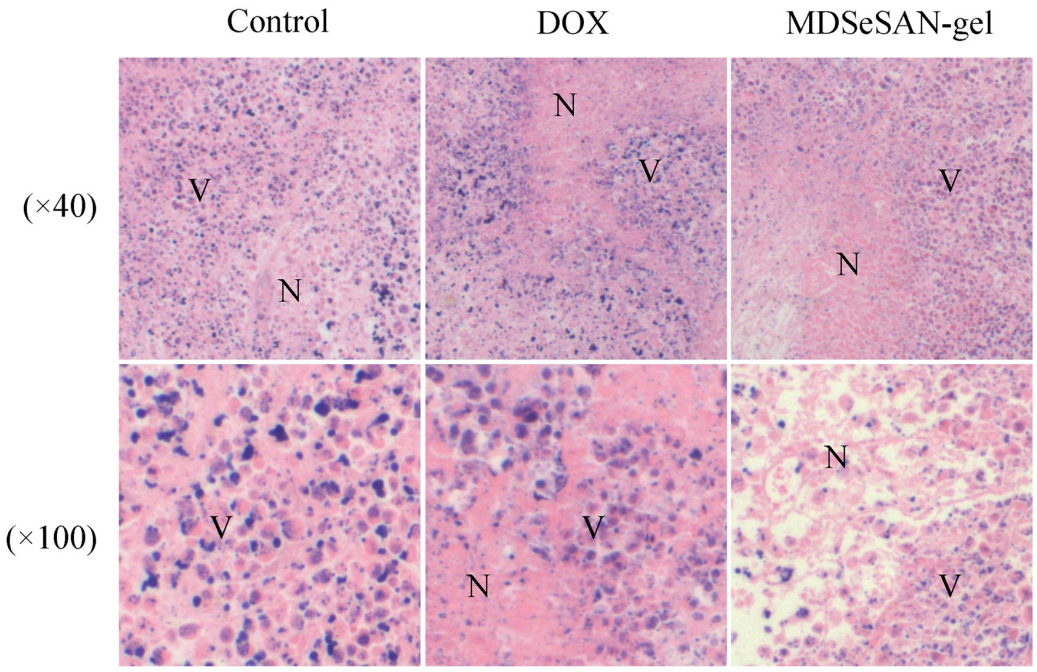

Fig S6. Representative images of tumor sections for the confirmation of antitumor activity by H&E staining. Necrotic cells (N); Viable cells (V).

To confirm the antitumor efficacy induced by this targeted therapy, Fig S6 showed the H&E staining of the tumor samples following treatment with control (PBS), DOX and MDSeSAN-gel, respectively. The necrotic regions (N) were identified by their darker pink color. Compared to the control or the PBS treated group, necrotic regions were typically observed within the tumor samples of mice treated with DOX and MDSeSAN-gel. Notably, MDSeSAN-gel treatment induced more remarkable necrosis in the tumors, where the most extensive necrotic centers and the least viable tumor cells were identified. Necrotic cells heterogeneously appeared as well throughout the whole tumor sections in the groups treated with DOX. These findings indicated that both DOX and MDSeSAN-gel had an inhibitory effect against the growth of H22 liver tumor cells *in situ*. This roughly exhibits that the nanogel presents high targeting

effect, perhaps due to the fact that the nanogel can only be effectively triggered to release under the specific environments at the tumor site.

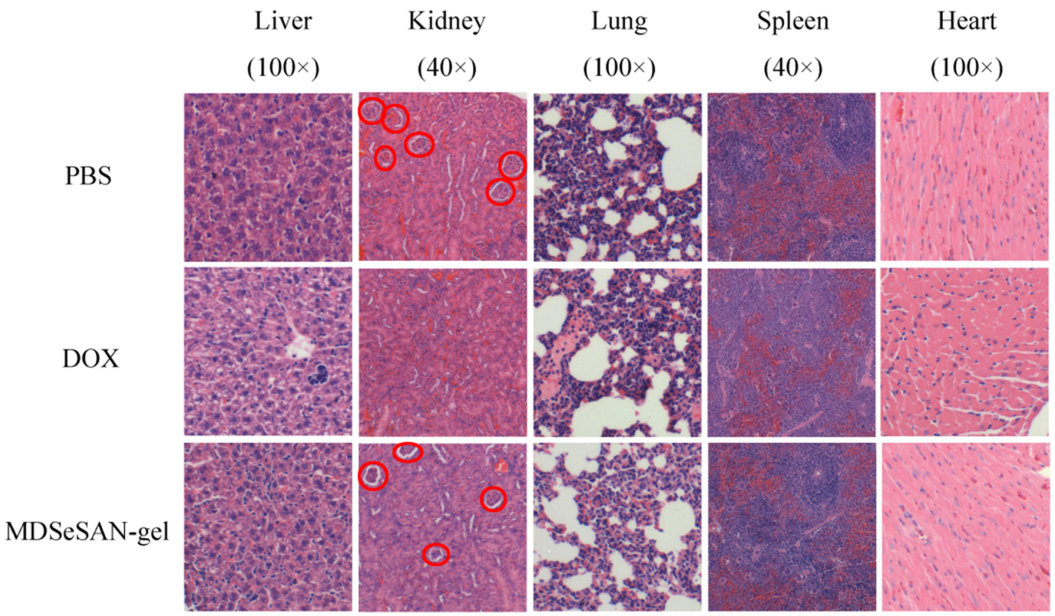

Fig S7. Histological assessments of tissue sections of vital organs.

The histological assessments of tissue sections of vital organs were carried out among the nanogel, free DOX and PBS groups to figure out the systemic adverse effect. In Fig S7, H&E staining of the liver tissues in PBS and MDSeSAN-gel groups revealed normal hepatocytes, central veins, portal triads and liver lobules. In contrast, DOX induced significant degeneration and apoptosis of liver cells, expressing obvious hepatotoxicity. Normal Bowman's capsules, marked in red circle, surrounding glomeruli as well as convoluted tubules were apparently observed in the PBS and MDSeSAN-gel groups. However, these structures were hardly identified in the free DOX group. Thus serious nephrotoxicity in the free DOX group turned out in kidney.

Normal alveoli without the sign of pulmonary fibrosis were found in the lung sections in the three groups, but the free DOX group displayed significant pulmonary congestion. No apparent difference was identified among the three groups in spleen samples. It was well known that anthracyclines usually cause cardiotoxicity. Visual evidence of myocardium tissue necrosis in heart sections was visually evident by the administration of DOX. Encouragingly, compact cardiac myocytes lined up in order with clear structure in the MDSeSAN-gel treated group. This is in close accordance with the PBS treated group, indicating that there were no histopathological abnormalities in both groups. This observation supported again the point that the nanogel will produce lower systemic adverse effect. This can be attributed to the fact the controlled leakage or release in the normal tissues, as expected. All above mentioned investigations indicated that the MDSeSAN-gel exhibits toxicity as low as PBS but higher therapy than free DOX.

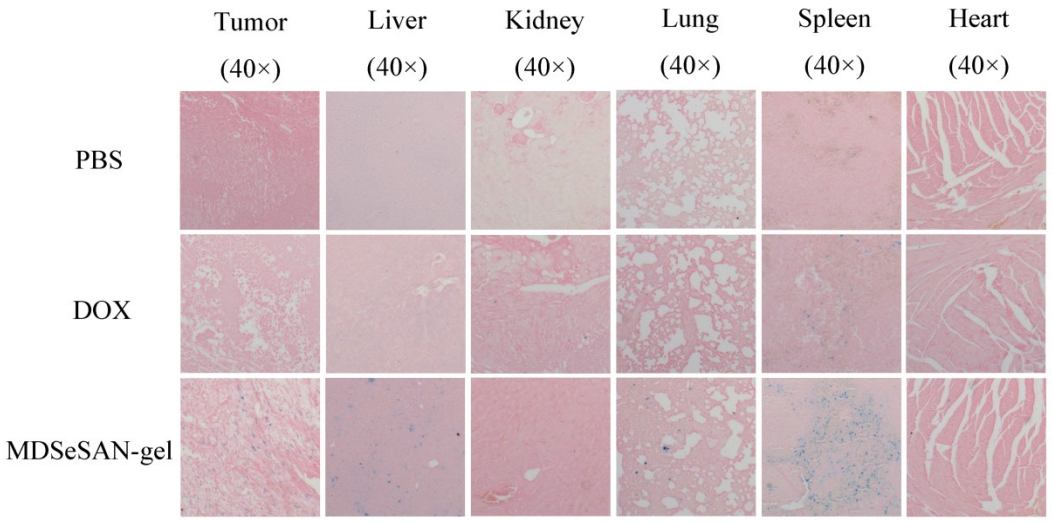

Fig S8. Tissue slice of mice treated with PBS, DOX and MDSeSAN-gel.

The *in vivo* accumulation and distribution of the MDSeSAN-gel were confirmed, as shown in Fig S8. Prussian blue staining was utilized to track the existing of iron or the MDSeSAN-gel. After the whole treatment, obvious accumulation of MDSeSAN-gel (indicated in blue dots) was observed in the tumor tissue. This clearly confirms the effective targeting of the MDSeSAN-gel or a high uptake in tumor. In vital organ sites, the staining results showed that the uptake of the nanogel in the liver, lungs and spleen was greater than the uptake in the heart and kidneys. This result was in agreement with the previous histological assessments of tissue sections of vital organs in Fig S7.

References

(1) Cheng, G.; He, Y.; Xie, L.; Nie, Y.; He, B.; Zhang, Z.; Gu, Z. Development of a Reduction-Sensitive Diselenide-Conjugated Oligoethylenimine Nanoparticulate System as a Gene Carrier. *Int. J. Nanomed.* **2012,** *7*, 3991-4006.

(2) Wang, Y.; Xu, H.; Ma, N.; Wang, Z.; Zhang, X.; Liu, J.; Shen, J. Block Copolymer Micelles as Matrixes for Incorporating Diselenide Compounds: a Model System for a Water-Soluble Glutathione Peroxidase Mimic Fine-Tuned by Ionic Strength. *Langmuir* **2006**, *22*, 5552-5555.

(3) Steinmann, D.; Nauser, T.; Koppenol, W. H. Selenium and Sulfur in Exchange Reactions: a Comparative study. *J. Org. Chem.* **2010**, *75*, 6696-6699.

(4) Huang, J.; Xue, Y.; Cai, N.; Zhang, H.; Wen, K.; Luo, X.; Long, S.; Yu, F. Efficient Reduction and pH co-Triggered DOX-loaded Magnetic Nanogel Carrier Using

Disulfide Crosslinking. *Mat. Sci. Eng. C-Mater.* **2015**, *46*, 41-51.

(5) Yu, F.; Huang, Y.; Cole, A. J.; Yang, V. C. The Artificial Peroxidase Activity of Magnetic Iron Oxide Nanoparticles and its Application to Glucose Detection. *Biomaterials* **2009**, *30*, 4716-4722.

(6) Wu, B.; Yu, P.; Cui, C.; Wu, M.; Zhang, Y.; Liu, L.; Wang, C. X.; Zhuo, R. X.; Huang, S. W. Folate-Containing Reduction-Sensitive Lipid-Polymer Hybrid Nanoparticles for Targeted Delivery of Doxorubicin. *Biomater. Sci.* **2015**, *3*, 655-664.

(7) Xue, Y.; Xia, X.; Yu, B.; Luo, X.; Cai, N.; Long, S.; Yu, F. A Green and Facile Preparation Technique of Alginate Nanogel as pH-Responsive Subcellular Delivery of Doxorubicin. *RSC Adv.* **2015**, *5*, 73416-73423.

(8) Song, M.; Xue, Y.; Chen, L.; Xia, X.; Zhou, Y.; Liu, L.; Yu, B.; Long, S.; Huang, S.; Yu, F. Acid and Reduction Stimulated Logic "and"-Type Combinational Release Mode Achieved in DOX-Loaded Superparamagnetic Nanogel. *Mat. Sci. Eng. C-Mater.* **2016**, *65*, 354-363.

(9) Song, M.; Xue, Y.; Lin, X.; Xia, X.; Chen, L.; Zhang, L.; Yu, B.; Long, S.; Huang, S.; Yu, F. Achievement of Release Mode under Combinational Stimuli by Acid and Reduction for Reduced Adverse Effect in Antitumor Efficacy. *Macromol. Mater. Eng.* **2016**, *301*, 1255-1266.

(10) Ding, J.; Chen, J.; Li, D.; Xiao, C.; Zhang, J.; He, C.; Zhuang, X.; Chen, X. Biocompatible Reduction-Responsive Polypeptide Micelles as Nanocarriers for Enhanced Chemotherapy Efficacy in Vitro. *J. Mater. Chem. B.* **2013**, *1*, 69-81.

(11) Ding, J.; Xu, W.; Zhang, Y.; Sun, D.; Xiao, C.; Liu, D.; Zhu, X.; Chen, X.

Self-Reinforced Endocytoses of Smart Polypeptide Nanogels for "on-Demand" Drug Delivery. *J. Control. Release.* **2013**, *172*, 444-455.

(12) Durmus, Z.; Kavas, H.; Toprak, M. S.; Baykal, A.; Altınçekiç, T. G.; Aslan, A.; Bozkurt, A.; Coşgun, S. L-Lysine Coated Iron Oxide Nanoparticles: Synthesis, Structural and Conductivity Characterization. *J. Alloy. Compd.* **2010**, *484*, 371-376.

(13) Bautista, M. C.; Bomati-Miguel, O.; Morales, M. D. P.; Serna, C. J.; Veintemillas-Verdaguer, S. Surface Characterisation of Dextran-Coated Iron Oxide Nanoparticles Prepared by Laser Pyrolysis and Coprecipitation. *J. Magn. Magn. Mater.* **2005**, *293*, 20-27.

(14) Zhang, H.; Xue, Y.; Huang, J.; Xia, X.; Song, M.; Wen, K.; Zhang, X.; Luo, X.; Cai, N.; Long, S. Tailor-Made Magnetic Nanocarriers with pH-Induced Charge Reversal and pH-Responsiveness to Guide Subcellular Release of Doxorubicin. *J. Mater. Sci.* **2015**, *50*, 2429-2442.

(15) Chen, L.; Xue, Y.; Xia, X.; Song, M.; Huang, J.; Zhang, H.; Yu, B.; Long, S.; Liu, Y.; Liu, L. A Redox Stimuli-Responsive Superparamagnetic Nanogel with Chemically Anchored DOX for Enhanced Anticancer Efficacy and Low Systemic Adverse Effects. *J. Mater. Chem. B.* **2015**, *3*, 8949-8962.